Liquid Crystals
Publication details, including instructions for authors and subscription information:
http://www.informaworld.com/smpp/title~content=t713926090

Structure and liquid crystalline properties of 5-[(4'-heptoxy-4-biphenylyl)carbonyloxy]-1-pentyne

Jianxin Geng[a]; Shuyun Wang[a]; Wei Ling[a]; Gao Li[a]; Enle Zhou Corresponding author[a]; Jacky Wing Yip Lam[b]; Benzhong Tang[b]
[a] State Key Laboratory of Polymer Physics and Chemistry, Changchun Institute of Applied Chemistry, Chinese Academy of Sciences, Changchun, PR China [b] Department of Chemistry, Hong Kong University of Science & Technology, Clear Water Bay, Kowloon, Hong Kong, PR China

Online publication date: 19 May 2010

To cite this Article Geng, Jianxin , Wang, Shuyun , Ling, Wei , Li, Gao , Zhou Corresponding author, Enle , Lam, Jacky Wing Yip and Tang, Benzhong(2004) 'Structure and liquid crystalline properties of 5-[(4'-heptoxy-4-biphenylyl)carbonyloxy]-1-pentyne', Liquid Crystals, 31: 1, 71 — 79
To link to this Article: DOI: 10.1080/02678290310001628519
URL: http://dx.doi.org/10.1080/02678290310001628519

LIQUID CRYSTALS, VOL. 31, NO. 1, JANUARY 2004, 71–79

Taylor & Francis
Taylor & Francis Group

Structure and liquid crystalline properties of 5-[(4′-heptoxy-4-biphenylyl)carbonyloxy]-1-pentyne

JIANXIN GENG, SHUYUN WANG, WEI LING, GAO LI, ENLE ZHOU*

State Key Laboratory of Polymer Physics and Chemistry, Changchun Institute of Applied Chemistry, Chinese Academy of Sciences, Changchun, 130022, PR China

JACKY WING YIP LAM and BENZHONG TANG

Department of Chemistry, Hong Kong University of Science & Technology, Clear Water Bay, Kowloon, Hong Kong, PR China

(*Received 19 December 2002; in final form 1 June 2003; accepted 16 August 2003*)

The crystal structure and liquid crystalline properties of a biphenyl-containing acetylene, [5-[(4′-heptoxy-4-biphenylyl)carbonyloxy]-1-pentyne (A3EO7) were investigated by electron crystallography, X-ray diffraction, polarizing optical microscopy, differential scanning calorimetry, transmission electron microscopy, and atomic force microscopy. A3EO7 crystals obtained from a toluene solution adopts a monoclinic $P112/m$ space group with unit cell parameters of $a=6.25$ Å, $b=7.82$ Å, $c=46.70$ Å and $\gamma=96.7^{\circ}$, as determined using electron diffraction. Upon cooling from the isotropic phase, A3EO7 exhibits a smectic A phase in the temperature range 72.4–53.6°C. Further lowering of the temperature results in the formation of a smectic C phase which exhibits a strong tendency towards crystallization.

1. Introduction

Almost all the side chain liquid crystalline polymers reported in the literature contain flexible backbones [1, 2], while those with rigid backbones have received little attention [3–8] owing to the general belief that rigid polymer backbones would disrupt the packing of the mesogens. This does not mean, however, that the stiffness of the backbone cannot be manipulated by appropriate molecular engineering of the molecular structures of the polymers, as we have shown by successfully developing a large number of mono-substituted and disubstituted liquid crystalline polyacetylenes [9–12]. We have systematically studied their materials properties and found that the polymers display unique electronic, optical, and mesomorphic properties originating from the synergistic interplay between the rigid backbones and the functional mesogenic pendants [13–15].

The study of the crystal structure and liquid crystalline (LC) properties of low molar mass acetylenes containing mesogenic groups is of importance because it enhances our understanding of the properties of the polymers. In previous work, we investigated the structure of an acetylene monomer, 11-[(4′-heptoxy-4-biphenylyl)carbonyloxy]-1-undecyne (A9EO7), and its polymer (PA9EO7) [16–18]. A9EO7 has an orthorhombic unit cell with cell constants of $a=5.78$ Å, $b=7.46$ Å, and $c=63.26$ Å, and belongs to the $P2_12_12$ space group. It displays monotropic LC behaviour, forming a smectic A (SmA) phase and two crystalline phases on cooling. Because of the rigidity of the polyacetylene backbone, the polymer PA9EO7, experiences difficulty in forming a three-dimensional lattice at room temperature and it shows SmA and smectic B phases on both heating and cooling. In another case, the polymer gives a high order smectic phase with a sandwich structure when prepared by the evaporation of a toluene solution.

To evaluate structure property relationships in biphenyl mesogenic moiety-substituted acetylene derivatives in a more detailed fashion, in this paper we describe the LC properties of another biphenyl-containing 1-alkyne with a short spacer length, 5-[(4′-heptoxy-4-biphenylyl)carbonyloxy]-1-pentyne (A3EO7), see figure 1. We found that A3EO7 packs in a

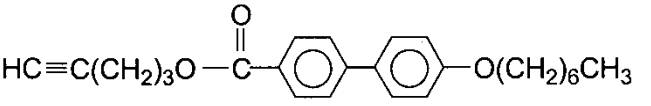

Figure 1. Molecular structure of A3EO7.

*Author for correspondence; e-mail: ydh@ns.ciac.jl.cn

Liquid Crystals ISSN 0267-8292 print/ISSN 1366-5855 online © 2004 Taylor & Francis Ltd
http://www.tandf.co.uk/journals
DOI: 10.1080/02678290310001628519

monoclinic fashion and exhibits monotropic SmA and smectic C (SmC) phases.

2. Experimental

2.1. *Characterization*

A Perkin-Elmer differential scanning calorimeter (DSC) was used to study the phase transitions. An Opton polarizing optical microscope (POM) equipped with a hot stage was used to observe the optical textures in cross-polarizing mode. X-ray diffraction (XRD) patterns were recorded on a Rigaku D/max 2500 PC diffractometer at variable temperatures using 1.54056 Å CuK_α radiation. The morphologies and electron diffraction (ED) patterns of A3EO7 were obtained using a JEOL2010 transmission electron microscope (TEM) operated at 200 kV. A rotation and tilt holder was used to obtain different crystallographic projections of the unit cell. The tilt angle was adjusted until the ED pattern of a new zone appeared and the maximum tilting angle was $\pm 33^\circ$. Atomic force microscope (AFM) images were recorded using a SPA300HV AFM with an SPI3800 controller (Seiko Instruments Industry Co. Ltd) at room temperature.

2.1. *Specimen preparation*

Figure 1 shows the molecular structure of A3EO7. Its synthesis was reported previously [10]. Samples used for TEM measurements were prepared as follows. A3EO7 was dissolved in toluene to make a 0.1 wt% solution. The solution was dropped onto a thin carbon film that had been evaporated on the surface of freshly cleaved mica. After evaporation of the solvent, microcrystals of A3EO7 were obtained. The carbon film was floated off onto a water surface and the sample was lifted using 400 mesh copper grids. The structure of A3EO7 was then studied using TEM.

To study the effect of a magnetic field on the molecular arrangement of A3EO7, the microcrystals on the carbon-coated mica surface were heated up to their melting point, and then quickly transferred into a magnetic field. The sample was placed in a direction parallel to the magnetic field; thus A3EO7 crystallized in the presence of the magnetic field. After cooling to its crystalline state, the sample was transferred to a Cu grid and its structure was studied using TEM.

3. Results and discussion

3.1. *Crystal structure and morphology of A3EO7*

3.1.1. *Cell and space group*

The XRD pattern of A3EO7 powder crystals obtained from a toluene solution is shown in figure 2. It is apparent that the diffraction peaks in the low angle region have an integral multiple relationship, i.e:

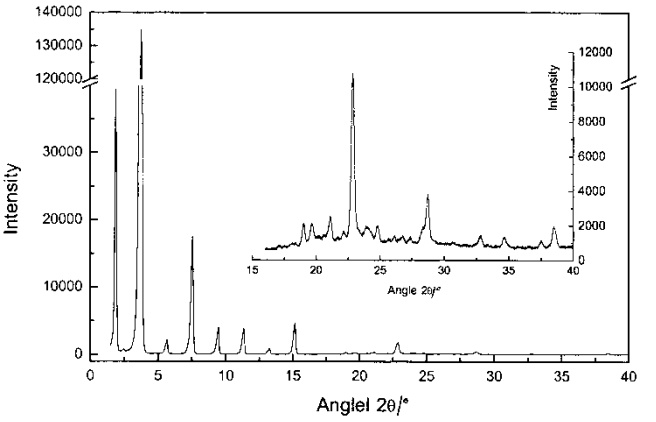

Figure 2. XRD pattern of A3EO7 in the crystalline state.

$d_1 = 2d_2 = 3d_3 = \ldots = nd_n = 46.70$ Å when $n \leqslant 8$ (n represents the sequence of diffraction peaks in the XRD pattern passing from the low angle to wide angle region). It is reasonable to conclude that the dimension of d_{001} is 46.70 Å. Since the molecular length of A3EO7 is approximately 24.5 Å, there must be two molecules packing in the c axis direction in a unit cell.

Figure 3 (*a*) shows the ED pattern of the basic zone or [0 0 1] zone of A3EO7 while figures 3 (*b*) and 3 (*c*) are the ED patterns after tilting the [0 0 1] zone by -4.8° and -6.4° around the a^* axis, respectively. The basic zone shows a rhombic two-dimensional pattern with dimensions of d_{100} of 6.21 Å and d_{010} of 7.76 Å, and a unit cell constant γ^* of 83.3°. The unit cell is thus triclinic or monoclinic. From the values of d_{100} and d_{010}, two molecules are also arranged in the unit cell in the direction of the a and b axes. Thus, there are four molecules in a unit cell. Now, there are only two molecules in one triclinic unit cell, [19], and therefore the unit cell is monoclinic.

Figures 3 (*b*) and 3 (*c*) are the ED patterns of the [0 1–2] and [0 2–3] zones, respectively. The unit cell constant c calculated from the tilting series of ED patterns is in agreement with the value obtained from the XRD pattern. As a result, the unit cell constants can be calculated as follows:

$$a = d_{100}[\cos(90 - 83.3)]^{-1} = 6.25 \text{ Å}$$

$$b = d_{010}[\cos(90 - 83.3)]^{-1} = 7.82 \text{ Å}$$

$$c = d_{001} = 46.70 \text{ Å}$$

$$a = \beta = 90^\circ \text{ and } \gamma = 96.7^\circ.$$

After determining the unit cell constants, the XRD pattern and all the ED patterns can now be indexed. The indexing of the XRD pattern is listed in table 1. In

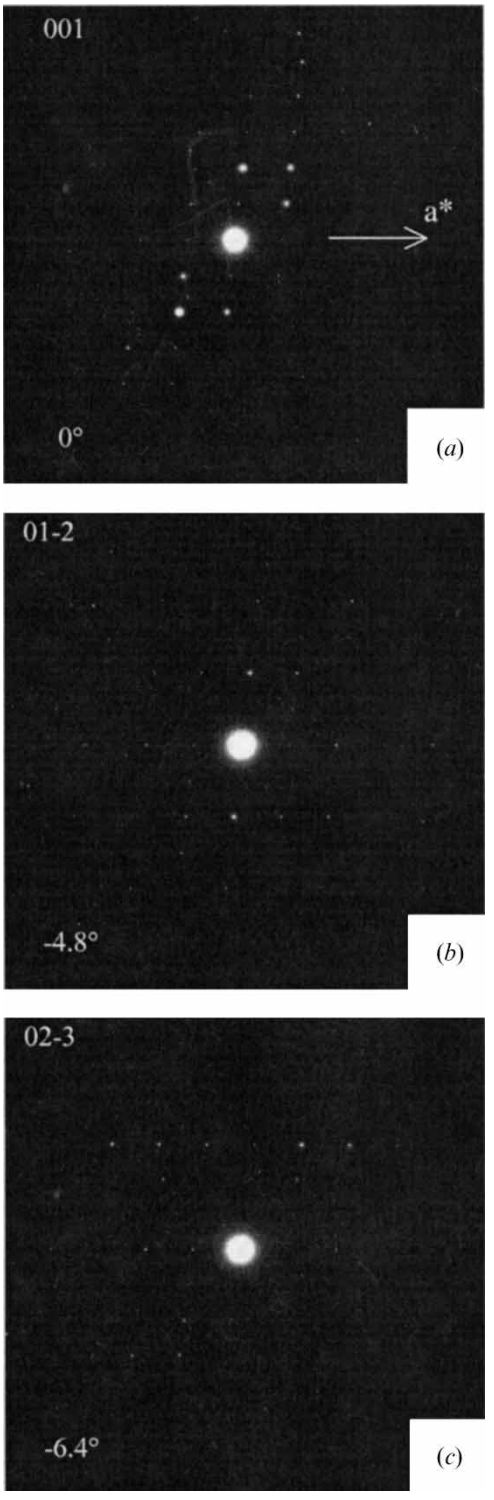

Figure 3. Tilt series of ED patterns of A3EO7 around the *a** axis. (*a*) [0 0 1] zone, (*b*) [0 1–2] zone and (*c*) [0 2–3] zone.

the analyses of the ED patterns and XRD pattern, no diffraction peaks are absent. By indexing using *International Tables for Crystallography*, the monoclinic lattice gives the lowest space group symmetry of *P*112/*m* and the calculated cell density is 1.11 g cm^{-3}.

Table 1. Index of the XRD pattern of A3EO7.

		d	
2θ/°	Index	Experimental	Calculated
1.89	0 0 1	46.70	46.70
3.77	0 0 2	23.42	23.35
5.67	0 0 3	15.57	15.57
7.57	0 0 4	11.68	11.68
9.47	0 0 5	9.31	9.34
11.35	0 0 6	7.79	7.78
13.27	0 0 7	6.67	6.67
15.19	0 0 8	5.83	5.84
19.02	0 1 8	4.66	4.67
19.68	1 1 2	4.51	4.51
21.09	0 0 1 1	4.21	4.24
22.88	0 2 0	3.88	3.88
24.81	0 2 5	3.59	3.59
28.73	2 0 0	3.10	3.10
32.81	2 1 3	2.73	2.73
34.64	0 3 0	2.59	2.59
38.49	−1 3 7	2.34	2.34

3.1.2. *Morphology study*

As shown in figure 4, crystals of A3EO7 exhibit a stepped layer morphology when observed under TEM. Since A3EO7 molecules possess a long heptoxy tail, the high molecular length to breadth ratio results in greater van der Waals forces between the in-cell molecules and neighbouring molecules when the unit cell is grown from the lateral side, than from the radial side. Thus the crystal has preferred growth in the lateral direction, resulting in a crystal with a layered structure. A similar morphology is also observed for A9EO7 [16]. It appears, therefore, that this crystallization behaviour

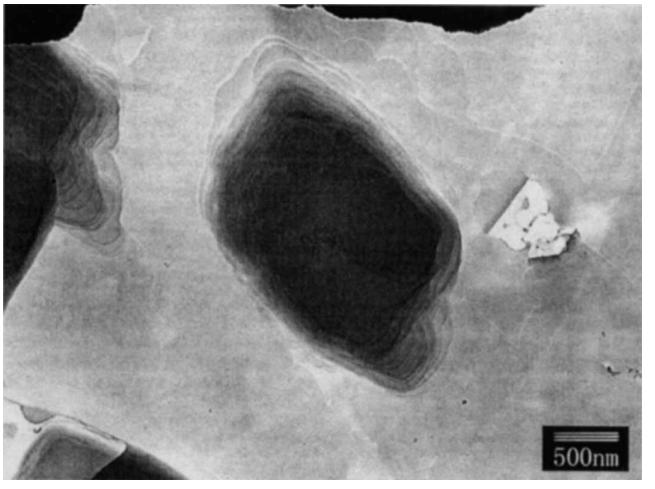

Figure 4. Stepped layer morphology of an A3EO7 crystal.

is common for 1-alkynes with biphenyl mesogen pendants. The thickness of the crystal layers can be estimated by AFM. As shown in Figure 5, the layer thickness is an integral multiple of the unit cell constant *c*. The direction of the molecular long axis is normal to the substrate because the molecular long axis is parallel to the *c* axis.

In previous work, we were able to induce A9EO7 to crystallize with its molecular long axis parallel to the substrate using a magnetic field [16]. The same approach also works for A3EO7. Figure 6 shows the morphology of A3EO7 obtained under the influence of a magnetic field. A3EO7 crystallizes in the direction of the applied magnetic field, as confirmed by the [0 0 l] reflections in the ED pattern, see figure 6 inset. The layer thickness seems to be larger than that without a magnetic field when comparing the contrast of the two images.

3.2. *LC properties of A3EO7*

3.2.1. *Phase transition and optical texture*

Figure 7 shows the DSC thermogram of A3EO7 recorded under the first cooling and second heating scans. Whereas three transition peaks are observed at 72.4, 53.6 and 35.6°C in the first cooling cycle, only one phase transition is detected, at 81.4°C, in the second heating cycle. The phase transition at 72.4°C corresponds to the isotropic to SmA phase transition and a characteristic focal-conic texture is readily observed when the isotropic melt is cooled to the corresponding temperature range under the microscope (figure 8). Further reduction of the temperature to 53.6°C results in the appearance of a broken focal-conic texture, indicative of the formation of a SmC phase. It is well known that the SmC phase exhibits two

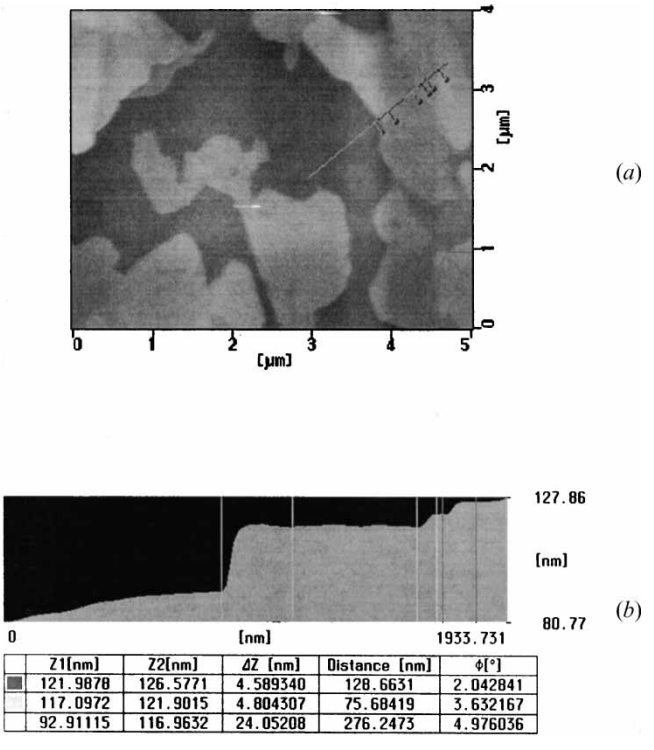

	Z1[nm]	Z2[nm]	ΔZ [nm]	Distance [nm]	Φ[°]
■	121.9878	126.5771	4.589340	128.6631	2.042841
	117.0972	121.9015	4.804307	75.68419	3.632167
	92.91115	116.9632	24.05208	276.2473	4.976036

Figure 5. (*a*) AFM image of A3EO7, (*b*) layer thickness of the crystal.

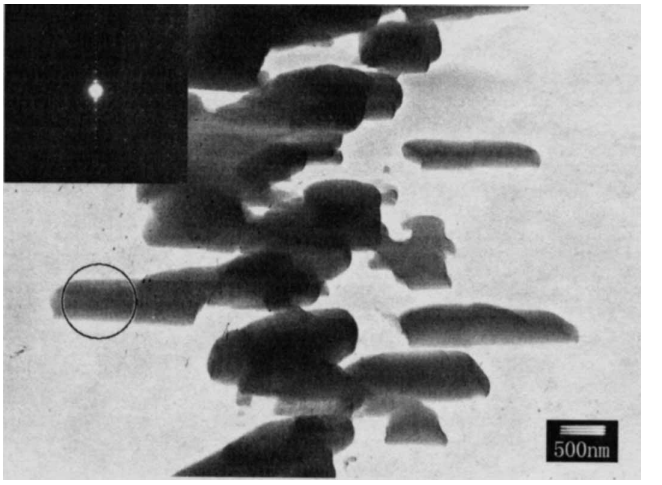

Figure 6. Morphology of A3EO7 crystal obtained under a magnetic field of 1 T. The inset shows the ED pattern.

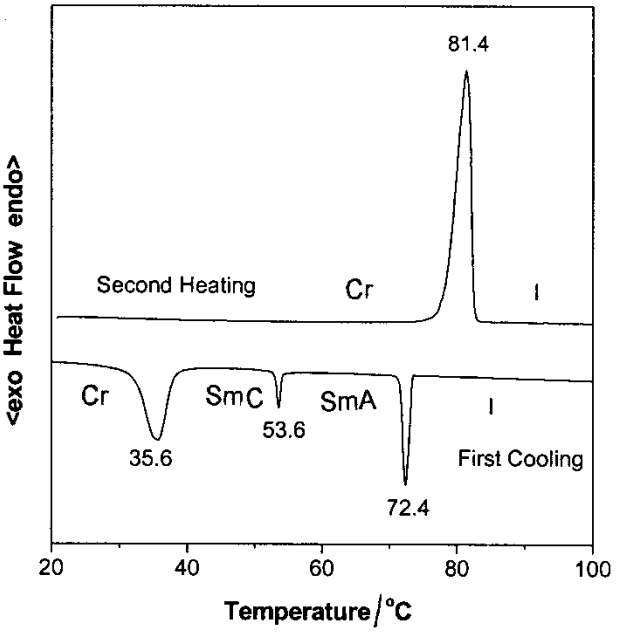

Figure 7. DSC thermograms of A3EO7 measured under nitrogen atmosphere at a scanning rate of 5°C min^{-1}. (Cr = crystalline state, SmA = smectic A phase, SmC = smectic C phase, I = isotropic state).

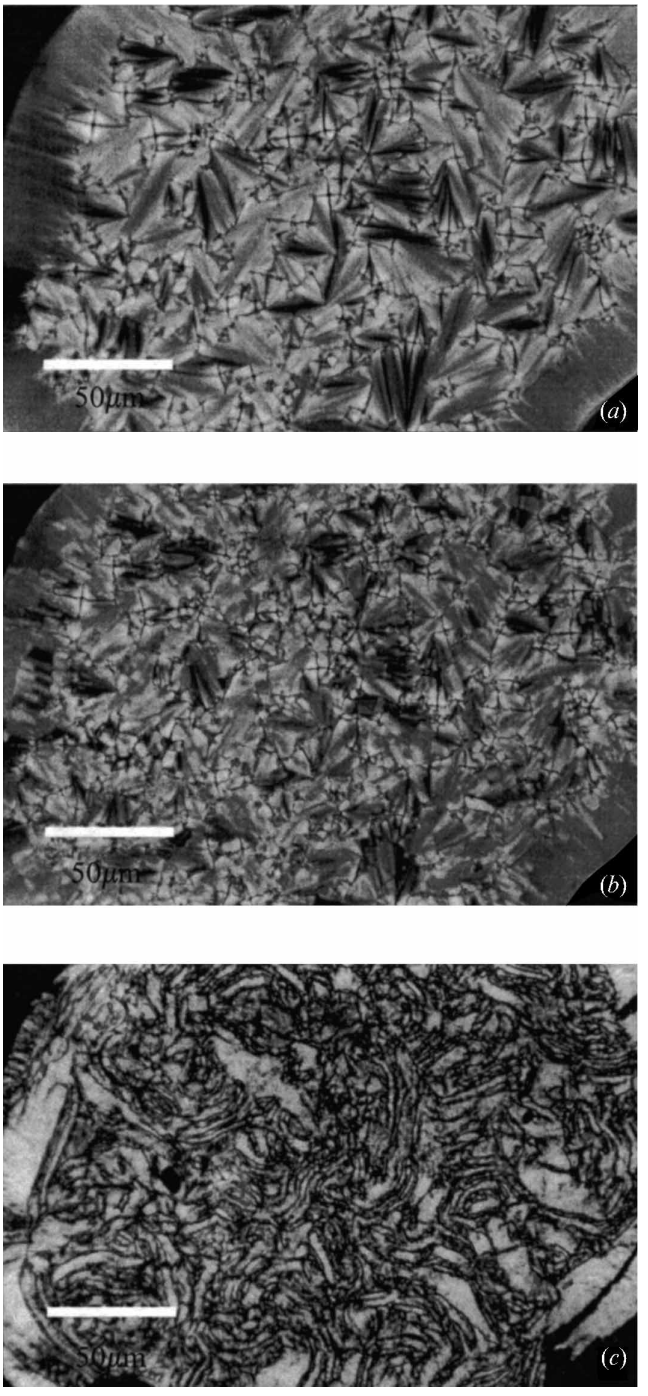

Figure 8. (*a*) Focal-conic texture of SmA phase observed at 68°C; (*b*) broken focal-conic texture of the SmC phase observed at 52°C; (*c*) crystal texture of A3EO7 obtained on cooling the sample from the isotropic melt.

characteristic textures, a schlieren texture and a focal-conic texture. But, if the SmC phase is exhibited on cooling a SmA phase, then the broken focal-conic texture will be obtained from the focal-conic texture of the preceding SmA phase [20]. A3EO7 crystallizes below 35.6°C; the crystal texture is shown in figure 8 (*c*). No LC texture is found in the second heating scan, showing that the LC behavior of A3EO7 is monotropic. Interestingly, A3EO7 also shows stepped drop and collapsed stepped drop textures in the temperature ranges 72.4–53.6°C and 53.6–35.6°C, respectively, when there is no glass slide covering the surface of the sample, see figure 9.

It is important to mention that once the broken focal-conic texture or collapsed stepped drop texture appears, it only exists for several minutes even if the temperature is held constant. This suggests that the SmC phase formed in the temperature range 56.3–35.6°C is Prone to crystallization. When the isotropic liquid of A3EO7 is cooled to a temperature at which the phase transition from the SmA phase to SmC phase is just complete, an exothermic peak

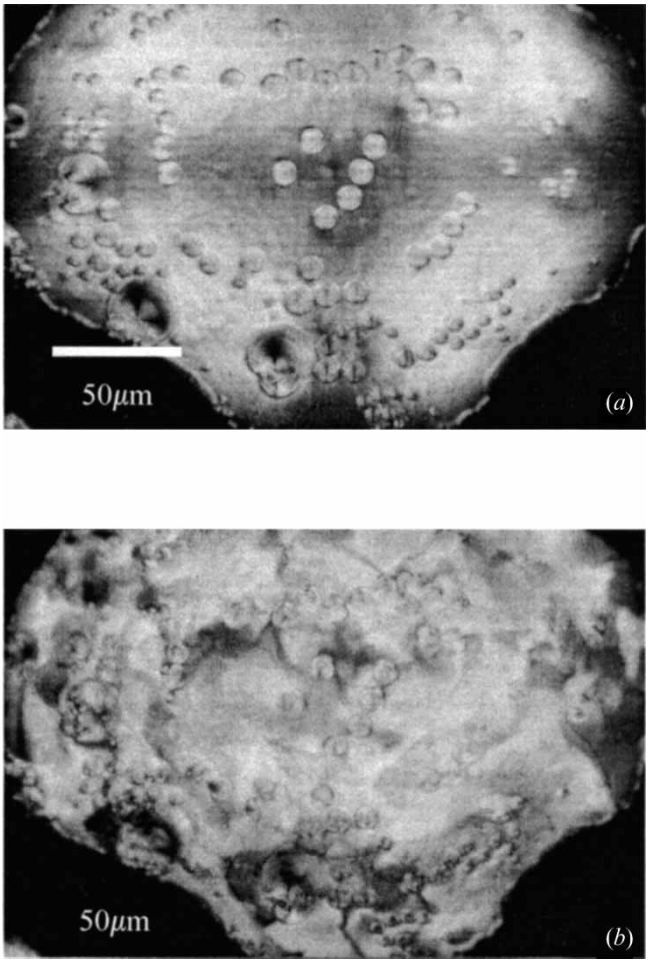

Figure 9. (*a*) Stepped drop texture of SmA phase observed at 66°C; (*b*) collapsed stepped drop texture of the SmC phase observed at 52°C when there is no glass cover on the sample, obtained by cooling the sample from its isotropic melt.

appears after holding at this temperature for ~ 2 min (figure 10). No peak corresponding to crystallization is detected when the temperature is further lowered. In a control experiment, where the temperature was kept at 65°C, i.e. the transition from the isotropic liquid to SmA is already complete, no peak was detected, even if the sample was annealed for 40 min (figure 11). On subsequent cooling the sample formed the SmC phase which in turn crystallized.

DSC thermograms recorded at different scanning rates are shown in figure 12. From the calculation of the temperature range of the unstable SmC phase and the

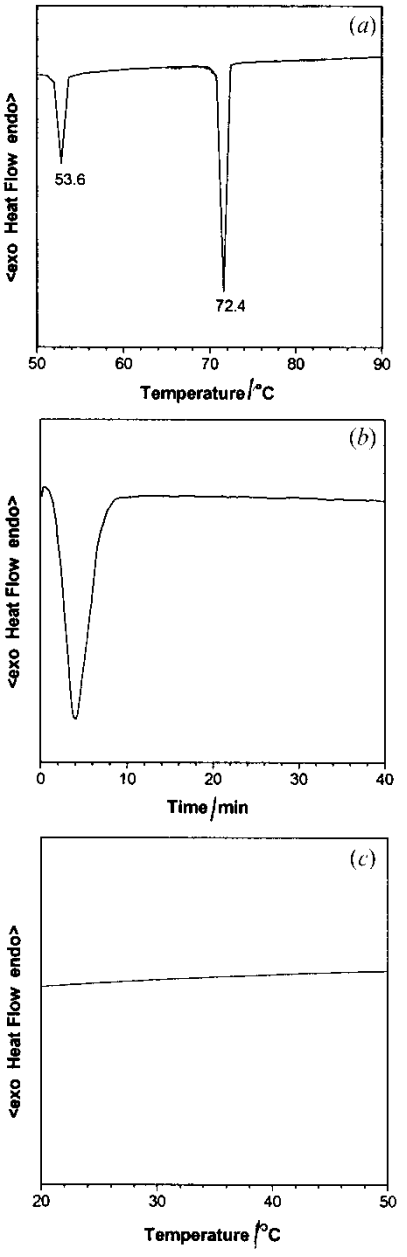

Figure 10. (*a*) DSC thermogram of A3EO7 obtained by cooling the sample from 120 to 50°C at which temperature the phase transition from SmA to SmC (see figure 7) is just complete; (*b*) heat flow *vs.* time curve when A3EO7 is kept at 50°C; (*c*) DSC curve on further cooling A3EO7 from 50°C to room temperature after annealing for 40 min.

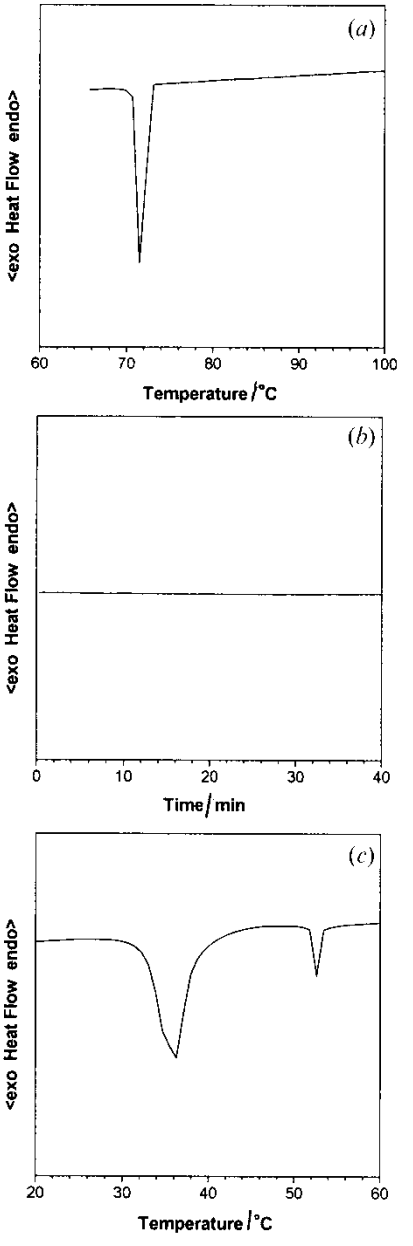

Figure 11. (*a*) DSC thermogram of A3EO7 obtained by cooling the sample from 120 to 65°C at which temperature the phase transition from isotropic phase to SmA (see figure 7) is complete; (*b*) heat flow *vs.* time curve when A3EO7 is kept at 65°C; (*c*) DSC thermogram of A3EO7 on cooling the sample from 65°C to room temperature, after annealing for 40 min.

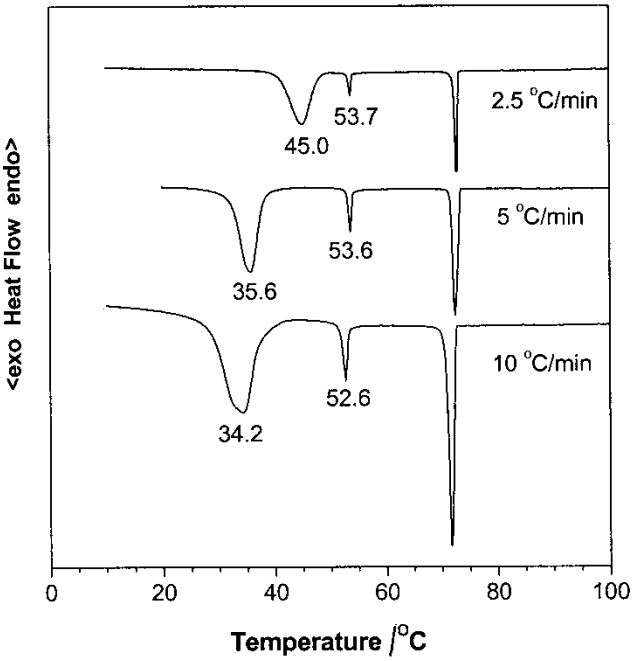

Figure 12. DSC cooling curve of A3EO7 measured at cooling rates of 2.5, 5 and 10°C min^{-1}.

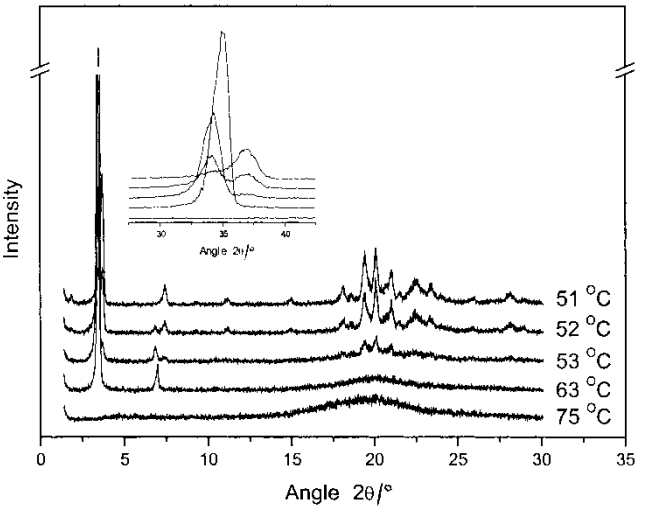

Figure 13. XRD pattern of A3EO7 at different temperatures obtained by cooling from the isotropic state.

scanning rate, the lifetime at the scanning rate of 2.5°C min^{-1} is equal to that at 5°C min^{-1}. But at a much faster scanning rate, 10°C min^{-1}, the lifetime becomes shorter. Therefore, the transition from the unstable SmC phase to the crystalline state is controlled not only by the temperature but also by the lifetime of the mesomorphic phase. The similar compound A9EO7 also exhibited an unstable phase, a crystal II phase, in our previous studies [17]. It appears that these unstable phases exhibited on cooling are an interesting phenomenon for 1-alkynes with biphenyl mesogens.

3.2.2. *Molecular arrangement in the liquid crystalline phase*

Figure 13 shows the XRD patterns of A3EO7 obtained at different temperatures. The diffractogram at 63°C shows a sharp reflection peak in the low angle region at $2\theta = 3.50°$, from which a *d*-spacing of 25.22 Å is derived using Bragg's law. This is associated with the distance between layer planes in the SmA phase. The reflection at an angle of $2\theta = 6.97°$ is the second order reflection. The diffuse halo centered at $\sim 20°$ ($d = 4.44$ Å) corresponds to the lateral intermolecular spacing. The molecular length of A3EO7 is calculated to be approximately 24.5 Å, suggesting the formation of a SmA phase.

The diffraction pattern at 53°C shows two sharp reflection peaks at $2\theta = 3.42°$ and 6.83°. In addition, two small reflection peaks are also detected at $2\theta = 3.69°$ and 7.41°. The *d*-spacing derived from the peaks at $2\theta = 3.42°$ is 25.81 Å which corresponds to the distance between layer planes in the SmC phase. The long range order in the SmC phase is 0.59 Å longer than that in the SmA phase, which may show that the preferred tilt angle between the molecular long axes of the constituent molecules and the normal to the layer planes in the SmC phase is smaller than the random tilt angle in the SmA phase. The peaks at $2\theta = 3.69°$ and 7.41° are, however, exactly where the diffraction peaks of (0 0 2) and (0 0 4) planes from the crystal appear at 51°C (in figure 13), the *d*-spacings of which are calculated to be 23.92 and 11.92 Å, respectively, from Bragg's law. When the temperature is lowered by 1°C, the reflection peaks at 3.42° and 6.83° become weaker and those at 3.69° and 7.41° become stronger compared with those seen at 53°C. The insert curve shows magnified reflection peaks in the low angle range. Because the transition from the unstable SmC phase to the crystalline state is partly controlled by time once the metastable LC phase appears, A3EO7 may start to crystallize during the measurement of the diffractograms at 53 and 52°C; a view supported by the crystalline peaks at higher angles. The diffractogram at 51°C is the XRD pattern of the crystalline state. Therefore, the diffractogram obtained at 53 and 52°C is a mixture of peaks from the SmC and crystalline phases. When the specimen is cooled to room temperature, the *d*-spacing of the (0 0 1) plane of the A3EO7 crystal is 47.70 Å, which is 1.00 Å longer than that of the crystal obtained from toluene solution. Table 2 gives the parameters of the long distance periodicities of the different phases.

As mentioned before, the A3EO7 crystal belongs to

Table 2. Long distance periodicities of A3EO7 in different phases.

Temperature/ °C	Phase	Stable or unstable	Long range order
72.4–53.6	SmA	Stable	25.22 Å
< 53.6	SmC	Unstable	25.81 Å
~ 50	Crystal (from melt)	Stable	47.84 Å
~ 25	Crystal (from melt)	Stable	47.70 Å
~ 25	Crystal (from solution)	Stable	46.70 Å

the *P*112/*m* space group with four molecules packing in one unit cell in an antiparallel manner. Although the molecules rearrange when the sample undergoes the phase transition from the crystalline state to LC phase, it is impossible that half of the molecules change their orientation so as to arrange in a parallel manner in the LC phase. Consequently molecules of A3EO7 must arrange in an antiparallel overlapping manner in the SmA and SmC phases (figure 14). The direction of the long axis of the biphenyl mesogens is on average normal to the layer planes in the SmA phase. The propyl spacer and the heptoxy tail are difficult to distinguish from each other owing to their random conformations. In the SmC phase, the molecular long axes of the constituent molecules tilt uniformly with respect to the normal to the layer planes.

4. Conclusions

The arrangement of the LC compound 5-[(4′-heptoxy-4-biphenylyl) carbonyloxy]-1-pentyne has been determined in the crystalline and LC phases. In the crystalline state, A3EO7 adopts a monoclinic *P*112/*m* space group with cell constants $a = 6.25$ Å, $b = 7.82$ Å, $c = 46.70$ Å and $\gamma = 96.7°$.

Crystals of A3EO7 show a multilayer morphology, the thicknesses of the layers being integral multiples of the cell parameter *c*. Molecules crystallize with their molecular long axis normal to the substrate. They, however, can be induced to lie parallel to the substrate by the application of a magnetic field.

Two LC phases, are found when A3EO7 is cooled from the isotropic melt. The stable monotropic mesophase, seen in the temperature range 72.4–53.6°C, is a smectic A phase with a layer spacing of $d = 25.22$ Å. The metastable (with respect to its tendency to crystallize) mesophase below 53.6°C, which was found to exist only for several minutes, is determined to be a smectic C phase with a layer spacing of $d = 25.81$ Å.

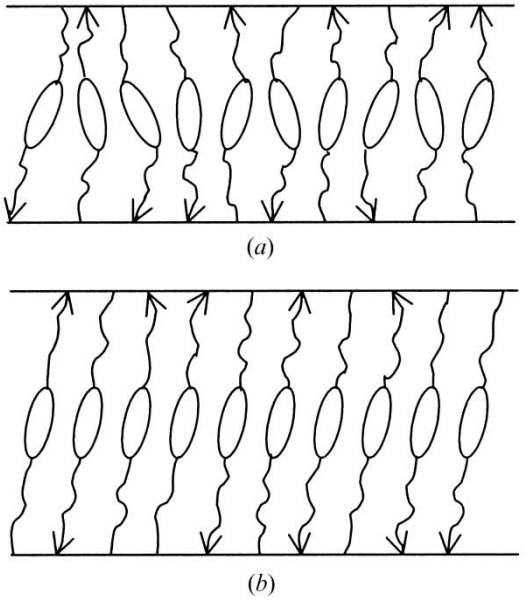

Figure 14. Packing arrangement of A3EO7 molecules in (*a*) SmA phase and (*b*) SmC phase.

We thank the National Natural Science Foundation of China (Project Nos: 29 904 008, 20 174 043 and 20 023 003) and the Research Grants Council of Hong Kong (Project Nos: HKUST6121/01P and 6085/02P) for financial support. This work was also subsidized by 'the Special Funds for Major State basic Research Projects'.

References

[1] McArdle, C. B., 1989, *Side Chain Liquid Crystal Polymers* (New York: Chapman & Hall).
[2] Collyer, A. A., 1992, *Liquid Crystal Polymers: from Structures to Applications* (New York Elsevier Applied Science).
[3] Akagi, K., and Shirakawa, H., 1996, *Macromol. Symp.*, **104,** 137.
[4] Choi, S. K., Gal, Y. S., Jin, S. H., and Kim, H. K., 2000, *Chem. Rev.*, **100,** 1645.
[5] Hasegawa, H., Kijima, M., and Shirakawa, K., 1997, *Synth. Met.*, **84,** 177.
[6] Kijima, M., Abe, S., and Shirakawa, H., 1999, *Synth. Met.*, **101,** 61.
[7] Osaka, I., Shibata, S., Toyoshima, R., Akagi, K., and Shirakawa, H., 1999, *Synth. Met.*, **102,** 1437.
[8] Osaka, I., Goto, H., Itoh, K., and Akagi, K., 2001, *Synth. Met.*, **119,** 541.
[9] Lam, J. W. Y., Luo, J., Dong, Y., Cheuk, K. K. L., and Tang, B. Z., 2002, *Macromolecules*, **35,** 8288.
[10] Lam, J. W. Y., Kong, X., Dong, Y. P., Cheuk, K. K. L., Xu, K., and Tang, B. Z., 2000, *Macromolecules*, **33,** 5027.
[11] Tang, B. Z., Kong, X., Wan, X., Peng, H., Lam, W. Y., Feng, X., and Kwok, H. S., 1998, *Macromolecules*, **31,** 2419.
[12] Tang, B. Z., Lam, J. W. Y., Kong, X., Lee, P. P. S., Wan, X., Kwok, H. S., Huang, Y. M., Ge, W., Chen, H., Xu, R., and Wang, M., 1999, in *Liquid Crystals III*, edited by I. Khoo (SPIE, Bellingham, WA), pp. 62–71.
[13] Tang, B. Z., Lam, J. W. Y., Kong, X., Salhi, F., Cheuk, K. K. L., Kwok, H. S., Huang, Y. M., and

GE, W., 2000, in *Liquid Crystals IV*, edited by I. Khoo (SPIE Bellingham, WA), pp. 24–30.
[14] TANG, B. Z., CHEN, H. Z., XU, R. S., LAM, J. W. Y., CHEUK, K. K. L., WONG, H. N. C., and WANG, M., 2000, *Chem. Mater.*, **12,** 213.
[15] KONG, X., and TANG, B. Z., 1998, *Chem. Mater.*, **10,** 3352.
[16] GENG, J., GENG, F., YANG, X., WANG, J., LI, G., ZHOU, E., and TANG, B., 2002, *Mol. Cryst. liq. Cryst.*, **383,** 115.
[17] GENG, J., GENG, F., WANG, J., ZHU, B., LI, G., ZHOU, E., LAM, J. W. Y., and TANG, B. Z. (submitted).
[18] GENG, J., ZHAO, X., ZHOU, E., LI, G., LAM, J. W. Y., and TANG, B. Z., 2003, *Mol. Cryst. liq. Cryst*, **339,** 17.
[19] HAHN, T., 1983, *International Tables for Crystallography* Vol. A (Boston: D. Reidel Publishing Co.), pp. 194–195.
[20] GRAY, G. W., and GOODBY, J. W. G., 1984, *Smectic Liquid Crystal-Texture and Structure* (Leonard Hill).